25th ABCM International Congress of Mechanical Engineering
October 20-25, 2019, Uberlândia, MG, Brazil

COB-2019-2393
IMPROVEMENTS IN MASKLESS ELECTROCHEMICAL SURFACE TEXTURING FOR CYLINDRICAL COMPONENTS

Gabriel Ferri
Leonardo Conde Dias
Henara Costa
Universidade Federal do Rio Grande, Campus Carreiros, Av Itália, km 8, Rio Grande – RS, Brasil
engenhariaferri@gmail.com
leonardocondedias@gmail.com
henaracosta@furg.br

Abstract. *The manufacture of micro dimple array is a proven way to improve lubrication in cylindrical sliding components. However, it remains a challenge to produce textured surfaces in large areas with low cost and texturing time, essential for industrial application and large-scale production of low-cost components. Maskless electrochemical texturing (MECT) draws attention as a very promising way of texturing low-cost components, such as sliding bearings and liners of combustion engines. This work proposes a new configuration for the texturing chamber used in MECT. A new apparatus was developed, where the electrolyte flows parallel to the textured region, in order to reduce the costs involved, improve the electrolyte flow and thus the efficiency of the process. Moreover, the use of an adhesive patterned mask was investigated as a way to create the insulation needed and avoid the tool perforation process. Voltages of 12V, with texturing times of 1, 3 and 5 min and a distance of 400 µm, allowed the manufacture of circular textures (650 to 1000 µm in diameter and 5 to 25 µm in depth) in low carbon steel cylindrical surfaces at very low cost.*

Keywords: *Surface texturing, cylindrical components, maskless electrochemical surface texturing.*

1. INTRODUCTION

The use of textured surfaces may provide better tribological characteristics regarding the performance of some mechanical systems. The modification of the surface topography generating a micro-relief with a controlled geometry is known surface texturing. Surface texturing with micro pockets is a known method for friction reduction in sliding contacts. In many cases, both wear and friction between two sliding surfaces can be reduced by texturing surfaces (Bruzzone et al., 2008). Various techniques have been developed in order to fabricate this type of surfaces. However, most fabrication methods have some limitation when the intention is to texture low cost components and large areas (Costa and Hutchings, 2015).

One of the most promising techniques to texture surfaces cheaply and fast is using localized electrochemical dissolution to selectively remove material of the surface. This localization of the anodic dissolution is often achieved using a mask on the specimen (Hsu et al., 2014). When the localization of the anodic dissolution is achieved via a mask on the tool (instead of on the specimen) it is called maskless electrochemical texturing (MECT) (Costa and Hutchings, 2009). Application of voltage pulses between an anode and a cathode in an electrochemical environment allows surface texturing with good precision at low cost. In addition, short texturing times and the possibility of texturing large areas make it a good candidate as a technique for low cost components. The use of ultrashort voltage pulses enhances the precision achieved by this method, since for shorter pulses the reactions are restricted to a region closer to the anode (Chen et al., 2015, Schuster et al., 2000). Different designs have been proposed for electrochemical texturing chambers. One approach involves micro electrochemical machining, where a tool electrode with small diameter (250 µm) and the workpiece are mounted to a three-axis positioning stage, immersed in an electrolyte. This technique dispenses the use of insulating masks, although an insulation layer could be used in the sidewall of the tool to minimize stray current. However, the texturing time is long because each pocket is machined individually (Byun et al., 2010). In through mask electrochemical micromachining (TMEMM) the insulation mask is clamped to the anode and the electrolyte flows between the cathode and the mask, as represented in Fig. 1 a, making it difficult to renew the electrolyte near the surface of the anode and making it necessary to mask all the pieces produced (Chen et al., 2015). A modified TMEMM has been proposed by Qian et al. (2010). In this configuration, the tool, which consisted of the cathode and the insulation layer, was put directly on the anode. Both the insulation layer and the tool have the same perforated patterns. This modified method can reduce the costs by eliminating the masking process of the workpieces alone, allowing one masked tool to perform several texturing cycles, it is represented in Fig. 1 b. However, electrolyte renewal remains hampered by the anode and insulation layers.

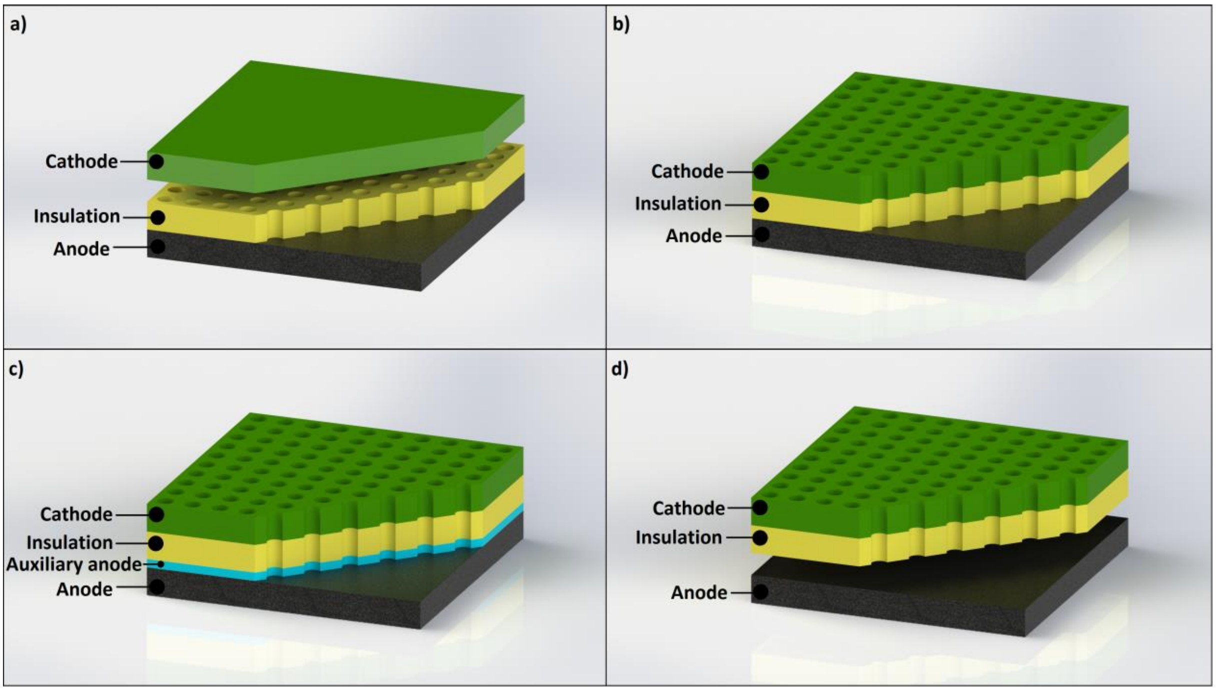

Figure 1. Comparison between different configurations of electrochemical texture.

Aiming to eliminate the lateral machining that occurs under the insulating mask and produce textures of higher lateral dimensions than the mask patterns, recently Qian et al. (2014) suggested the use of an auxiliary anode, represented by the Fig. 1 c. The localization of the material removed was improved with the auxiliary anode, although the costs are higher due to the consumption of the auxiliary anode during the process. In order to eliminate the masking costs, a configuration was proposed by Costa and Hutchings (2009). This arrangement, called maskless electrochemical texturing (MECT), allows the electrolyte to flow through the holes in the tool and then scape through the gap between the anode face and the insulation, enhancing the electrolyte renovation and the removal of the electrolysis products, represented by Fig. 1 d. Despite the great relation between costs and precision obtained by this technique, it is not commercially available yet (Gachot et al., 2017).

All the configurations shown can successfully generate textured surfaces in large areas with little time. In order to definitely eliminate the costs involved in the workpiece masking process and also eliminate the laborious tool perforation, this work suggests an adaptation in the MECT technique. The configuration suggested, represented by Fig. 2, allows the electrolyte to flow parallel to the cathode and anode faces, enabling higher electrolyte renovation in the textured face. Also, there is no need to insert the patterns in the cathode.

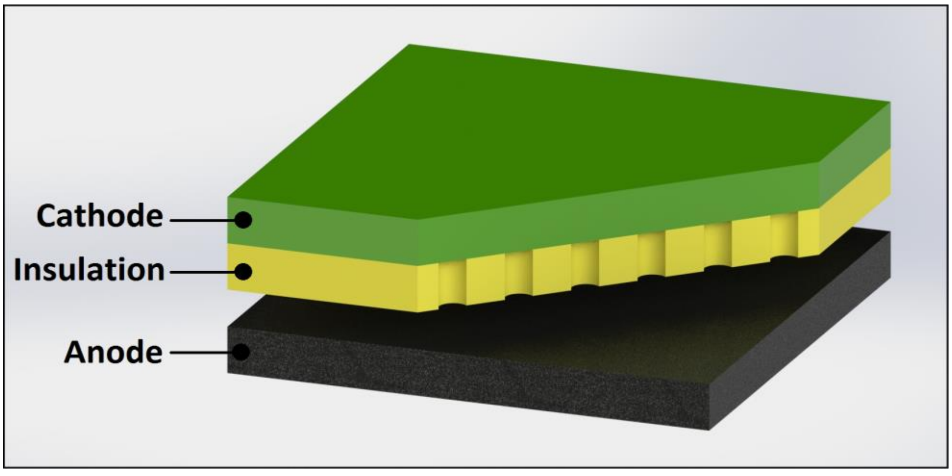

Figure 2. MECT modified configuration.

2. EXPERIMENTAL PROCEDURES

At first it was thought which parameters would be used to make surface texturing. Electrochemical texturing process performance is strongly influenced by the parameters involved. For example, small distance variation between the electrodes, flux and concentration of electrolyte, voltage and electric current, and texturing time can make efficient removal of material impossible. Since then, the design apparatus, tool and the samples, must be developed by considering all these parameters.

Initially, parameters referred in similar studies in the literature were selected. The 50Hz frequency was successfully used in the works of Parreira et al. (2012) and Costa and Hutchings (2009). A duty cycle of 20% was found to be more appropriate for machining larger depths in the works of Chen et al. (2015). The applied voltage has a format of a rectangular wave, with peaks and valleys duration of 4 ms and 16 ms respectively.

The distance between the electrodes is very important for that process. If shorter the distance between them, deeper will be the pockets machined for the same time, if the electrolyte flow is enough (Parreira et al., 2012). In that way was maintained constant the distance between the electrodes at 400 µm. The flux of electrolyte across of the texturing chamber is an answer of the apparatus arrangement.

2.1 Development of the experimental apparatus

A schematic representation of the texturing chamber developed is shown in Fig. 3. In this figure, the points 1 and 2 are respectively the connections for electrolyte inlet and outlet, the points 3 and 4 are holes through the nylon chamber till the workpiece or tool for accommodating electrical wires to enable electrical contact. The apparatus also had a power generator, which provided the energy needed for electrochemical machining at a specific voltage, frequency and pulse duty cycle. A pump and reservoir were used to promote the circulation of the electrolyte.

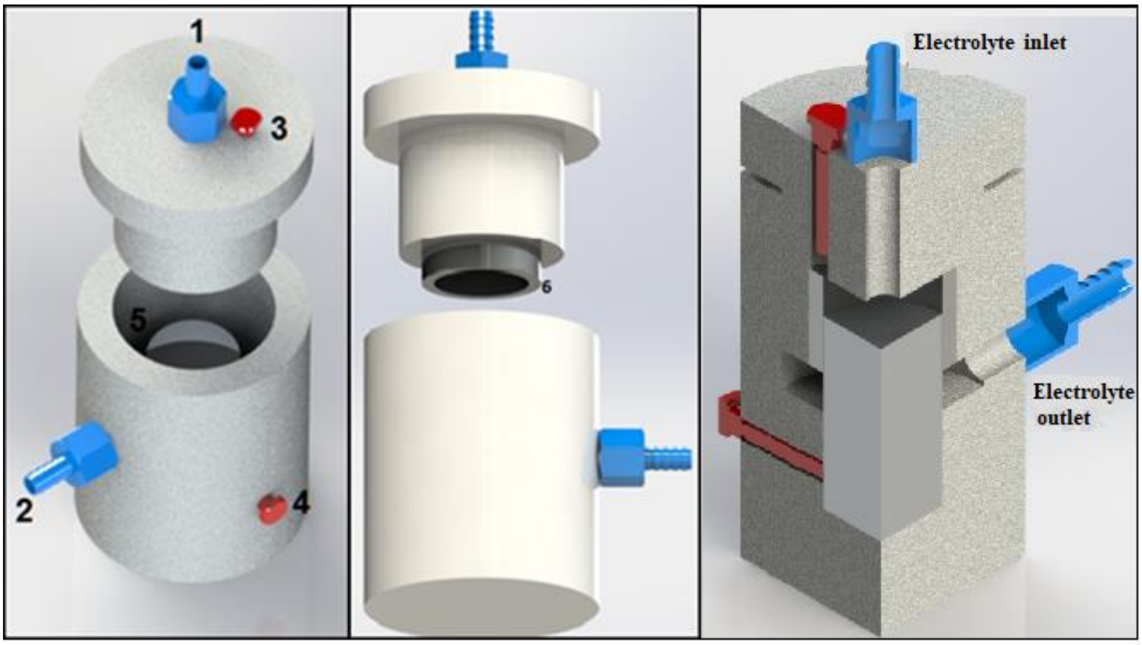

Figure 3. Texturing chamber.

2.2 Workpieces and tools manufacturing

The workpieces used were machined from an ABNT 1020 steel tube. The internal surface of the samples was polished with 2 µm diamond paste for 5 minutes at 400 rpm to achieve mirror-polished finish. Sample dimensions after cutting, machining and polishing are shown in Fig. 4. Since the area defined to be textured is approximately 40 mm², a single cylindrical sample may be used for various tests.

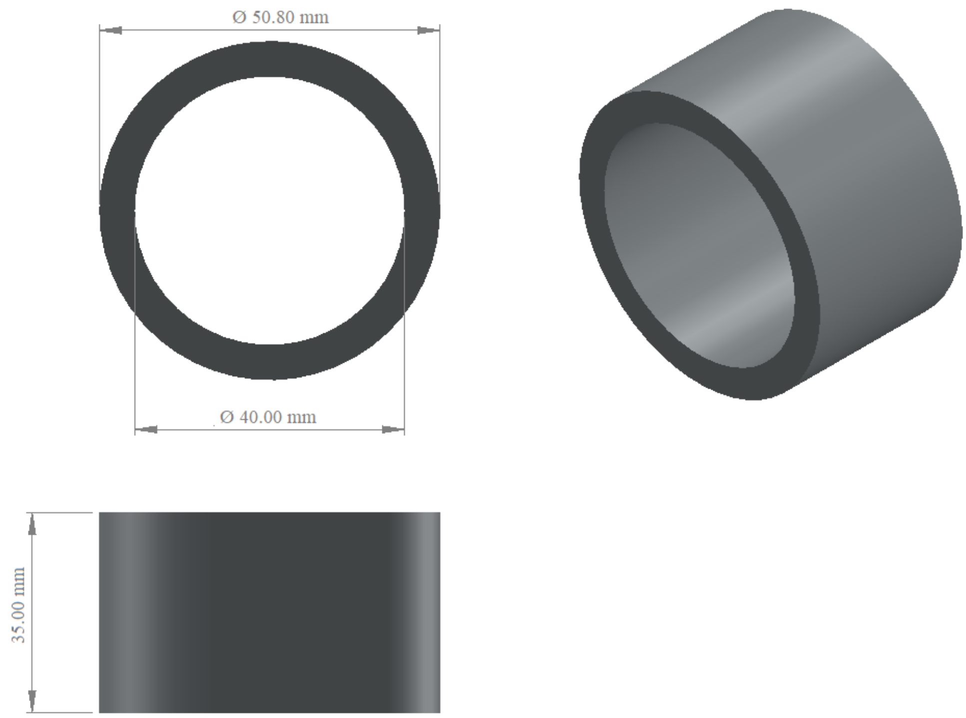

Figure 4. Sample final dimensions.

The tool was machined from a solid bar of AISI 316 stainless steel and polished to a mirror-finish. The final dimensions of the tools are represented in Fig. 5.

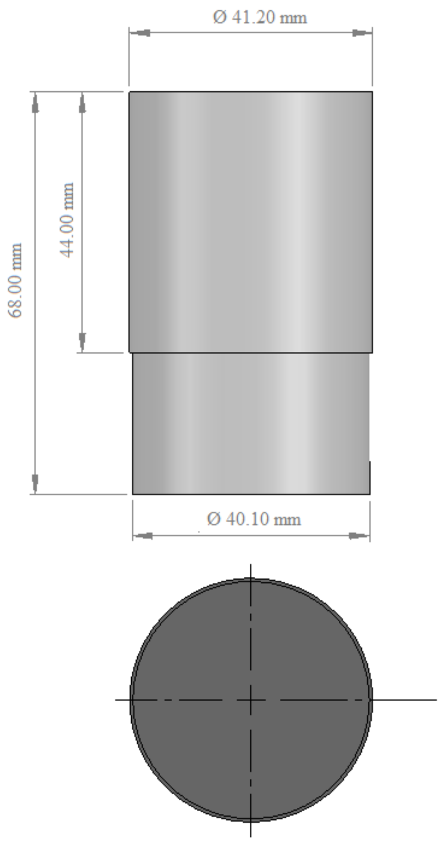

Figure 5. Tool final dimensions.

Without the insulation provided by the masking process, electrochemical machining would not be restricted to a small region, making the production of the regular patterns impossible. To produce the patterned insulation on the tool, it was covered with a laser-perforated adhesive. The measurements of the programmed laser perforation as well as the actual perforation performed on the adhesive are shown in Fig. 6. The other exposed metal parts of the tool were coated with insulating tape, exposing only the metallic area previously drilled in the adhesive. In this way the masking process was greatly simplified.

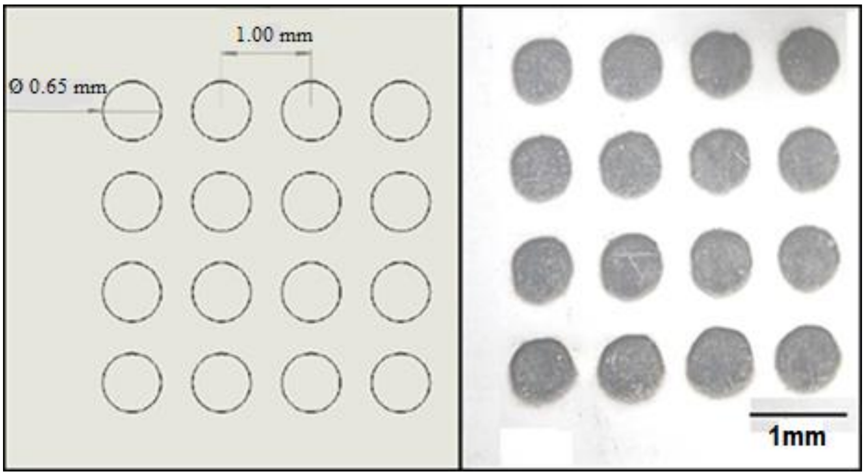

Figure 6. Programmed laser perforation (left) and perforation result (right).

2.3 Surface texturing experiments

The pulsing frequency was 50Hz, the duty cycle was 20%, the voltage was 12V, the distance between electrodes (gap) was 400 μm and the flow rate was 110 $ml.s^{-1}$. The electrolyte concentration and the machining time were varied for each test carried out according to Tab. 1. Concentrations of 2M, 3M and 4M NaCl in water were tested. In order to evaluate the performance of a solution containing $NaNO_3$ in combination with NaCl, 3 trials with 2M NaCl + 1M $NaNO_3$ in water were also carried out.

Tests were all performed using the same tool. After each test, the tool was repositioned in order to texture another region of the same cylindrical sample. The face of the tool was cleaned with cotton to remove any possible residue from the previous process. After texturing, the samples were polished for 2 minutes with 2 μm diamond paste at 400rpm rotation, so that the oxides formed on the surface were removed. Then the workpieces were cut into smaller samples, each representing a concentration per time of texturing, as shown in Fig. 7.

Table 1. Code of samples, concentrations and times used in surface texturing tests.

Machining time	NaCl 2M	NaCl 3M	NaCl 4M	NaCl 2M + $NaNO_3$ 1M
1 minute	1A	4A	7A	1C
2 minutes	2A	5A	8A	2C
3 minutes	3A	6A	9A	3C

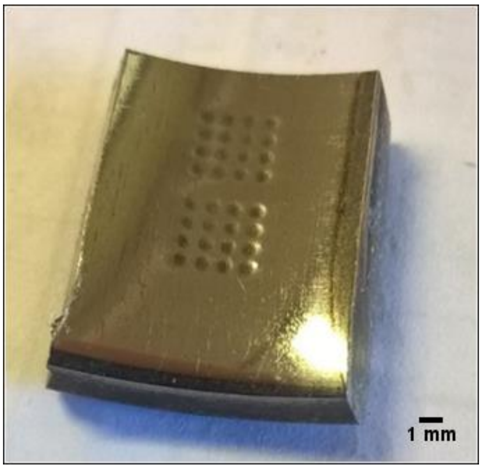

Figure 7. Section of a textured cylindrical sample.

The measurements of the depth and profile of the pockets were performed using a Bruker profilometer, ContourGT and the software vision 64. The maximum depth mentioned in the results is an approximation of the maximum depth found with the software vision64, while de diameter is an approximation of the diameter shown after the use of a filter that allows only the region above the zero (the region not machined) to be shown. Observations by scanning electron microscopy was performed using a Jeol JSM-6610LV.

3. RESULTS AND DISCUSSION

The flux of electrolyte obtained with the new rig configuration was computed by measuring the time for a volume of 5 L of electrolyte to flow between the workpiece and the tool. This calculation gave an electrolyte flux of 110 ml.s -1, which is much higher than the values of 20 $ml.s^{-1}$ and 3 $ml.s^{-1}$ shown in the literature for the previous versions technique (Costa and Hutchings, 2009). Such increase must result from the fact that the fluid flows parallel between the workpiece and the tool instead of through holes in the tool cover, which must substantially reduce head losses. However, it must be emphasized that the gap size used in this work was larger, which must also have contributed to increase the flux of electrolyte.

A result of the profile measurement and the depth of the machined sample for one minute with a mixture of 2M NaCl and 1M $NaNO_3$ is presented in Fig. 8 for one pocket. It has good circularity, with a concave profile, typical of electrochemical machining. All pockets machined during the texturing tests showed a similar profile, with maximum depths ranging from 5 to 25 μm.

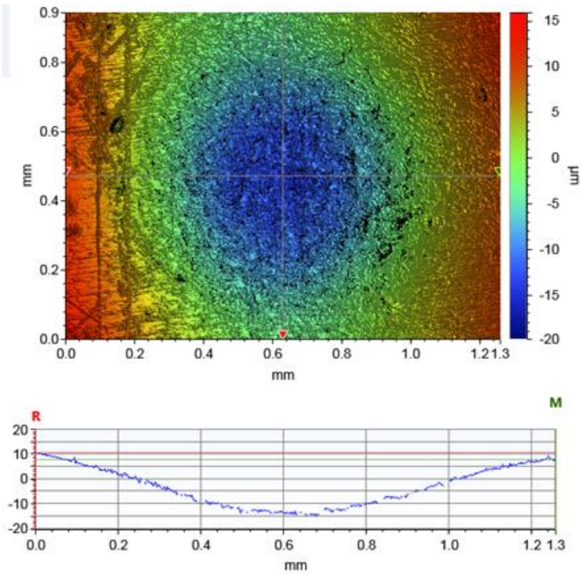

Figure 8. Pocket typical profile.

The results of the evaluation of the maximum depth of the textures by profilometry are summarized in Fig. 9. Both the increase of time and concentration resulted in deeper pockets. However, the influence of concentration was stronger for the shortest texturing time. The sample machined for 1 min with a mixture of 2M NaCl and 1M $NaNO_3$ showed a maximum depth of approximately 14 µm. This depth was higher than that found in samples machined with 2M and 3M NaCl without the addition of $NaNO_3$. However, for longer machining times, the advantage of mixing with $NaNO_3$ has not been verified.

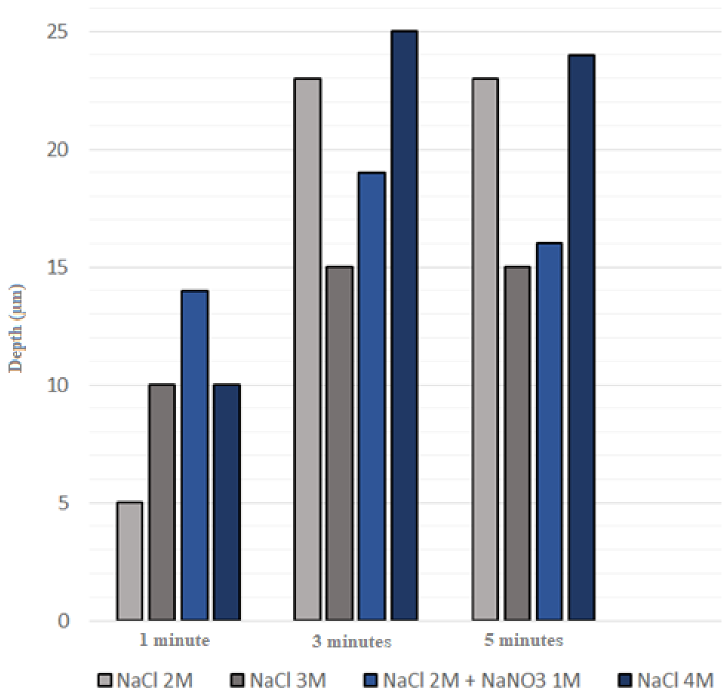

Figure 9. Pocket maximum depth.

Machining is not limited to the region immediately perpendicular to the exposed metal zone of the tool. It occurs that an adjacent region also ends up having material removed, with less intensity, resulting in pockets and textures of larger lateral dimensions than those established in the tool by masking. Thus, after a certain time, electrochemical machining tends to significantly increase the lateral dimensions of the pockets, without causing a considerable depth increase. This behavior was also verified in Parreira et al. (2012) and (da Silva and Costa, 2017).

Figure 10 shows the average diameter of the machined pockets. It can be verified that the concentration does not have a great influence on the resulting diameter for the machined pockets, since the factor of greatest impact was the texturing time. The increase in machining time from 1 minute to 5 minutes resulted in a maximum difference of approximately 300 µm in diameter and 19 µm in depth. In this way it is evident that one should opt for smaller times in order to obtain textures of reduced lateral dimensions, more faithful to the masking pattern.

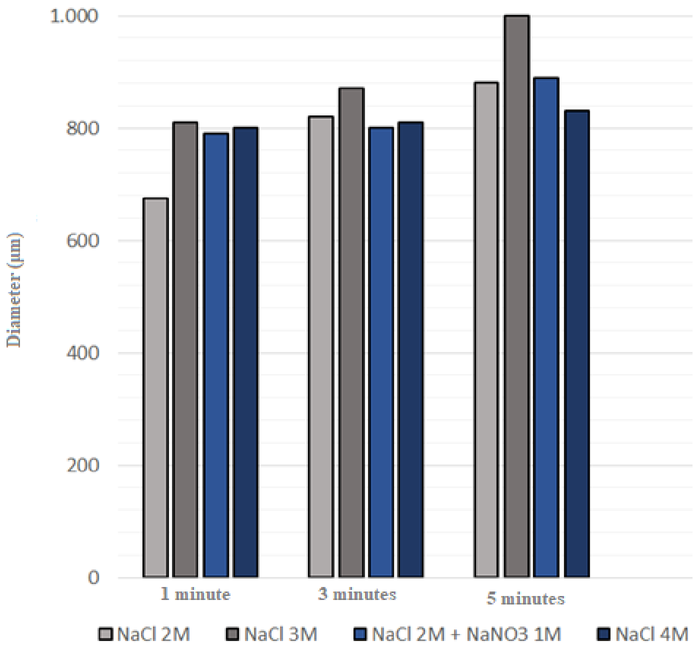

Figure 10. Estimated pocket diameters.

Figure 11 refers to a sample machined for 1 min, with little machining in the region between the pockets. Figure 12 refers to a sample machined for 5 min, which had severe material removal in the region between the pockets, practically providing fusion between them. In those images, all the regions of a reference plane (zero) were digitally removed using the software, so that only the regions above the reference plane are visible, corresponding to the regions that theoretically did not have material removed during the texturing process. This high removal of material between the pockets is the factor that prevents to obtain textures with deeper pockets for larger texturing times.

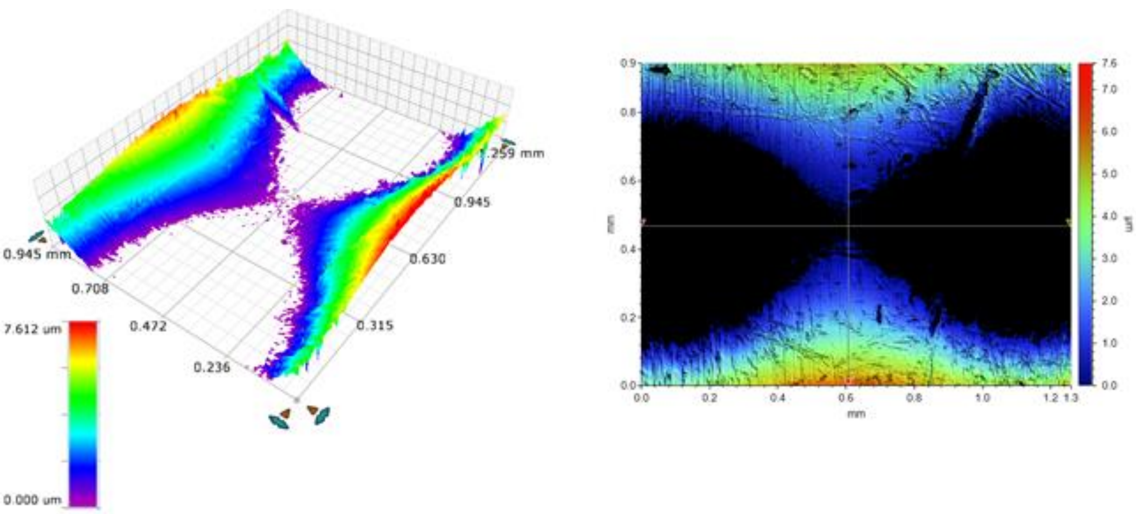

Figure 11. Profilometry image of the region between the pockts of a sample machined for 1 min.

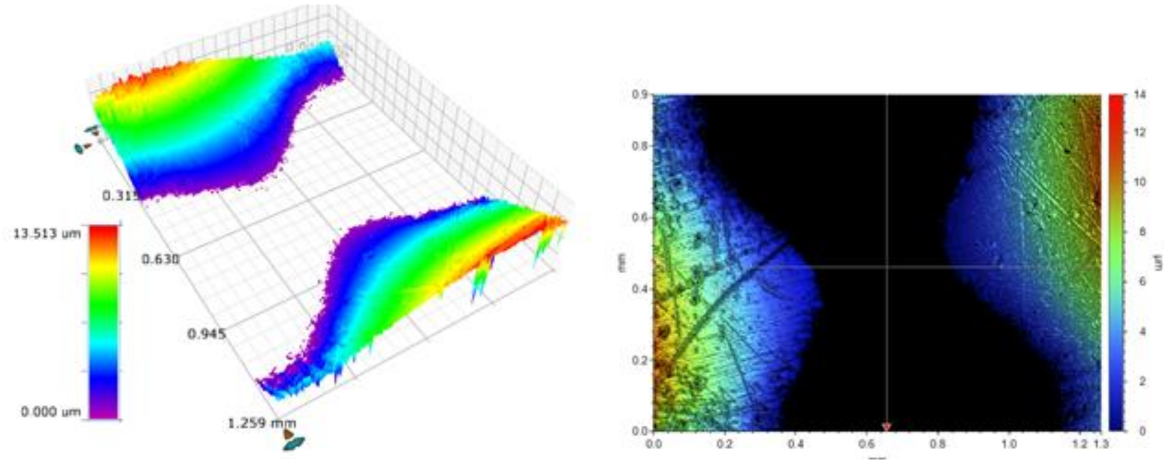

Figure 12. Profilometry image of the region between the pockets of a sample machined for 5 min.

Fig. 13 shows SEM images of the textures produced. The region denoted as 2, which was practically not machined during the process, has a much lower amount of exposed carbon than region 1, inside the pocket, which had approximately 15µm of material removed. It is necessary to remember that region 2 was also polished after machining. The higher amount of carbon present in the dark regions suggests a preferential dissolution of the ferrite relative to the cementite. In addition, it is possible that material removed from mask could be incorporated into the surface of the pockets. In the texturing of gray cast iron by MECT in da Silva and Costa (2017), was observed that the electrochemical machining removed the metal matrix exposing the graphite. This effect played a favorable role, since the graphite ended up acting as a solid lubricant.

Summarizing, this work proposed and evaluated a new design for surface texturing chambers. It improved the electrolyte flow when compared to other configurations presented in the literature. It enabled the production of arrays of pockets in cylindrical surfaces, although the minimum pocket diameter was around 650 µm. On the other hand, it should be noted that masks contained smaller holes could be easily obtained, reducing the dimensions of the final pockets.

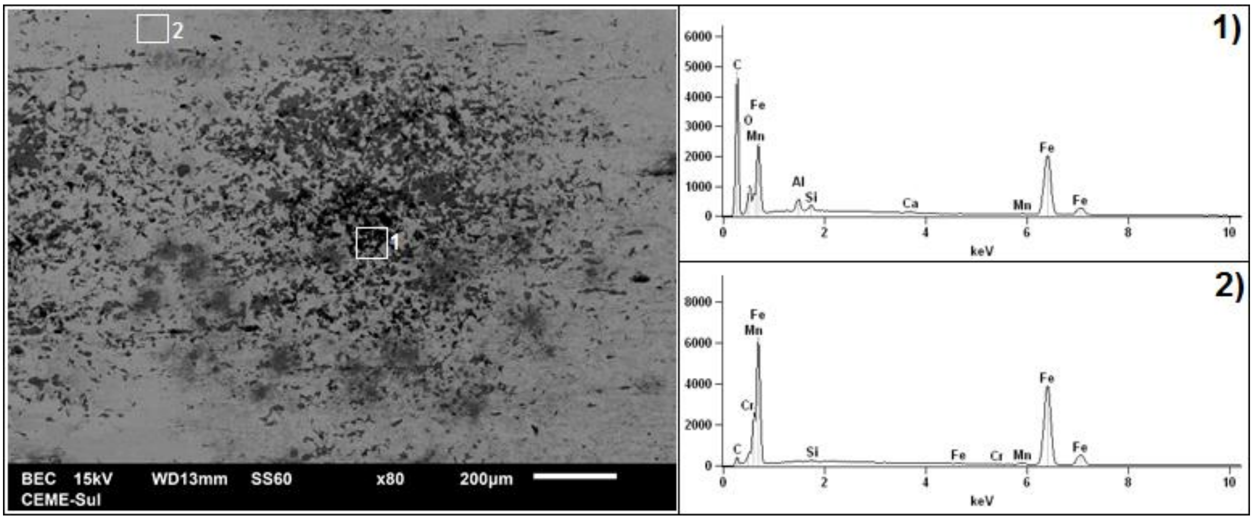

Figure 13. SEM image and EDS of regions 1 and 2.

4. CONCLUSIONS

It was possible to elaborate an apparatus accessible and efficient to texturing cylindrical components for low carbon steel, the dimensions of the pockets produced are similar that found in the literature. To the dimensions available, the use of an adhesive mask proved to be cheap and efficient way to replace the masking of the tools.

High electrolyte concentration (NaCl 4M) in combination with short texturing times (1 minute), shown the most favorable results. For longer texturing times, the influence of the electrolyte concentration on the maximum depth was negligible. Longer machining times induced high removal of material between the pockets.

A voltage of 12 V, with texturing times of 1 minute together a gap size between the electrodes of 400 μm, allowed the manufacture texture patterns containing dimples with 800 μm in diameter and 10 μm in depth. All the pockets showed a concave profile.

The electrochemical machining changes the chemical composition of the surface region, probably resulting from the preferential dissolution of the ferrite relative to the cementite.

5. REFERENCES

Bruzzone, A. A. G., Costa, H. L., Lonardo, P. M. and Lucca, D. A. (2008) "Advances in engineered surfaces for functional performance", *Cirp Annals-Manufacturing Technology*, 57(2), pp. 750-769.

Byun, J. W., Shin, H. S., Kwon, M. H., Kim, B. H. and Chu, C. N. (2010) "Surface texturing by micro ECM for friction reduction", *International Journal of Precision Engineering and Manufacturing*, 11(5), pp. 747-753.

Chen, X. L., Qu, N. S., Li, H. S. and Xu, Z. Y. (2015) "Pulsed electrochemical micromachining for generating micro-dimple arrays on a cylindrical surface with a flexible mask", *Applied Surface Science*, 343, pp. 141-147.

Costa, H. L. and Hutchings, I. M. (2009) "Development of a maskless electrochemical texturing method", *Journal of Materials Processing Technology*, 209(8), pp. 3869-3878.

Costa, H. L. and Hutchings, I. M. (2015) "Some innovative surface texturing techniques for tribological purposes", *Proceedings of the Institution of Mechanical Engineers Part J-Journal of Engineering Tribology*, 229(4), pp. 429-448.

da Silva, L. R. R. and Costa, H. L. (2017) "Tribological behavior of gray cast iron textured by maskless electrochemical texturing", *Wear*, 376, pp. 1601-1610.

Gachot, C., Rosenkranz, A., Hsu, S. M. and Costa, H. L. (2017) "A critical assessment of surface texturing for friction and wear improvement", *Wear*, 372, pp. 21-41.

Hsu, S. M., Jing, Y., Hua, D. and Zhang, H. (2014) "Friction reduction using discrete surface textures: principle and design", *Journal of Physics D-Applied Physics*, 47(33).

Parreira, J. G., Gallo, C. A. and Costa, H. L. (2012) "New advances on maskless electrochemical texturing (MECT) for tribological purposes", *Surface & Coatings Technology*, 212, pp. 1-13.

Qian, S. Q., Ji, F., Qu, N. S. and Li, H. S. (2014) "Improving the Localization of Surface Texture by Electrochemical Machining with Auxiliary Anode", *Materials and Manufacturing Processes*, 29(11-12), pp. 1488-1493.

Qian, S. Q., Zhu, D., Qu, N. S., Li, H. S. and Yan, D. S. (2010) "Generating micro-dimples array on the hard chrome-coated surface by modified through mask electrochemical micromachining", *International Journal of Advanced Manufacturing Technology*, 47(9-12), pp. 1121-1127.

Schuster, R., Kirchner, V. V., Allongue, P. and Ertl, G. (2000) "Electrochemical micromachining", *Science*, 289(5476), pp. 98-101.

6. RESPONSIBILITY NOTICE

The author(s) is (are) the only responsible for the printed material included in this paper.